

## THICKNESS DISTRIBUTION OF ILLITE CRYSTALS IN SHALES. II: ORIGIN OF THE DISTRIBUTION AND THE MECHANISM OF SMECTITE ILLITIZATION IN SHALES

TERESA DUDEK\* AND JAN ŚRODOŃ

Institute of Geological Sciences, Polish Academy of Sciences, Senacka 1, 31-002 Kraków, Poland

**Abstract**—The distributions of illite crystal ('fundamental particle') thickness in <0.2  $\mu\text{m}$  fractions of 13 shale samples (from the Carpathian Foredeep, Poland), obtained using the Bertaut-Warren-Averbach X-ray diffraction method (MudMaster computer program), were analyzed and interpreted in terms of the mechanism of smectite illitization. All illite crystal thickness distributions in the analyzed shales are characterized by an 'asymptotic' shape. The origin of the asymptotic-type distributions is explained by the heterogeneity of illite crystals in shales, *i.e.* superposition of different populations of crystals, those included in illite-smectite (I-S) interstratifications, and those which occur as discrete illite. The analysis of the distributions in shales shows that the most frequent thickness class of illite crystals forming I-S is 2 nm. Discrete illite is composed of thicker crystals; though crystals as thin as 2 nm can also contribute to this population. The modeling of asymptotic distributions in shales by using a number of theoretical lognormal distributions shows that with progressive diagenesis, the mean thickness of illite crystals forming the I-S component increases gradually, whereas the discrete illite does not show a clear trend.

The diverse origins of illite crystals in shales do not permit determination of the mechanism of smectite illitization from the evolution of the shape of the overall crystal-thickness distribution during diagenesis. Therefore, in order to understand the mechanism of smectite illitization in shales, an attempt was made to trace the relative gains and losses of crystals of different thicknesses during illitization. This approach indicates the following mechanism of smectite illitization in the investigated shales: dissolution of smectite monolayers accompanied by growth of 2 nm crystals which are largely of detrital origin. Nucleation of 2 nm illites seems to be very limited.

**Key Words**—Crystal-size Distribution, Diagenesis, Illite, Fundamental Particles, Illite-smectite, Lognormal Distribution, Shales, Smectite Illitization.

### INTRODUCTION

Mixed-layer I-S, a major component of fine-grained clastic rocks, is the main mineral indicator of the diagenetic evolution of sedimentary basins. The thorough application of I-S in basin analysis requires an understanding of the smectite-to-illite reaction mechanism. This mechanism has been studied extensively in bentonites, which usually represent simple systems, comprising pure diagenetic I-S. Today, many authors agree that smectite illitization in bentonites proceeds through a dissolution-crystallization mechanism (*e.g.* Clauer *et al.*, 1997; Drits *et al.*, 1996; Inoue and Kitagawa, 1994; Środoń *et al.*, 2000). However, bentonites are scarce and their application in basin analysis is limited. In shales, which are present in virtually all basins, the mechanism of smectite illitization is poorly understood because these rocks contain complex assemblages, comprising populations of illite crystals having different origins and ages.

One of the ways to gain insight into the smectite-to-illite reaction mechanism is an analysis of crystal-size distributions. The original approaches to crystal-size distribution analysis, such as the classical kinetic theory,

often provided unsatisfactory results (*e.g.* Kirkpatrick, 1981) or, like the empirical methods developed for chemical engineering and applied to rocks (*e.g.* Marsh, 1988), are limited generally to magmatic processes (*e.g.* Burkhard, 2002; Higgins, 2002). Eberl *et al.* (1998a) developed a new method of deducing the rates of nucleation and the growth mechanisms of crystals from the shapes of crystal-size distributions. The method of Eberl *et al.* (1998a), regarded as universal, is based on the prediction of theoretical shapes for crystal-size distributions by computer simulation (program GALOPER) of crystal nucleation and growth, using the following equations: the Law of Proportionate Effect, a mass-balance equation, and equations for Ostwald ripening. The growth mechanism of a real population of crystals is deduced by comparison of theoretical and experimental shapes of crystal-size distributions. Eberl *et al.* (1998a) recognized three basic shapes for size distributions of natural crystals: lognormal, asymptotic, and a universal steady-state shape. The authors also identified three different mechanisms for crystal growth which produced those shapes, *i.e.* surface-controlled growth, simultaneous nucleation and growth, and Ostwald ripening. In the strict sense, this approach models the evolution of crystal size of an individual sample during the reaction progress ( $\alpha$  and  $\beta^2$  plot of Eberl *et al.*, 1998a, see below). It can also be used to analyze the crystal growth mechanism from a set of

\* E-mail address of corresponding author: nddudek@cyf-kr.edu.pl

samples if they represent subsequent stages of a single crystallization event.

Starting from the pioneering work of Nadeau *et al.* (1984a, 1984b, 1985), a number of I-S studies concentrated on analyzing the smallest separable entities of I-S, so called 'fundamental particles', which were shown to be genetically related to mixed-layer crystals (MacEwan crystallites): fundamental particles (referred to in the present contribution as illite crystals and smectite monolayers) are the "building blocks" of MacEwan crystallites (Środoń *et al.*, 1990; Reynolds, 1992). It was assumed that the information on the illitization mechanism is locked in the shape of fundamental particles, and not the mixed-layer crystals.

Eberl and Środoń (1988), Inoue *et al.* (1988), Šucha *et al.* (1993) and Christidis (1995) investigated the illite crystal-size distributions in I-S from diagenetically or hydrothermally altered bentonites. They interpreted the distributions to follow a steady-state shape and pointed to Ostwald ripening as the most probable mechanism of growth of illite crystals. However, later studies revealed that lognormal distribution of crystal size is the most common distribution shape among minerals and prevails for authigenic illites and mixed-layer I-S from bentonites (Eberl *et al.*, 1990, 1998a, 1998b; Drits *et al.*, 1998; Środoń *et al.*, 2000). The modeling of the evolution of lognormal distributions by GALOPER indicated that the growth of illite crystals is surface-controlled, and does not proceed via the Ostwald ripening mechanism.

Theoretical lognormal distribution  $g(x)$  is defined as the distribution of a random variable  $x$ , whose logarithm is normally distributed:

$$g(x) = \frac{1}{x\beta\sqrt{2\pi}} \exp\left\{-\frac{(\ln x - \alpha)^2}{2\beta^2}\right\}$$

$$\text{For } x > 0, \text{ and } g(x) = 0 \text{ for } x \leq 0 \quad (1)$$

where  $\alpha$  and  $\beta^2$  are the distribution parameters that correspond to the mean value and variance of  $\ln x$ , respectively:

$$\alpha = \sum \ln x f(x) \quad (2)$$

$$\beta^2 = \sum [\ln x - \alpha]^2 f(x) \quad (3)$$

where  $f(x)$  describes the observed frequency of  $x$ , and  $x$  is the thickness of illite crystals.

Środoń *et al.* (2000) proposed the three-stage mechanism of smectite illitization in bentonites (Figure 1, open triangles): (1) nucleation of 2 nm illite crystals at the incipient stages of illitization, until I-S containing ~70% smectite monolayers is formed (at ~60–70%S as measured by XRD); (2) nucleation of 2 nm illite crystals at a decreasing rate accompanied by their growth until nearly all monolayers are consumed (up to ~30%S); nucleation dominates for  $R = 0$  I-S, which is evidenced by the asymptotic shape of crystal thickness distributions; for  $R > 0$  I-S, the growth of nucleated particles dominates, and the shape of distribution becomes lognormal; (3) surface-controlled growth

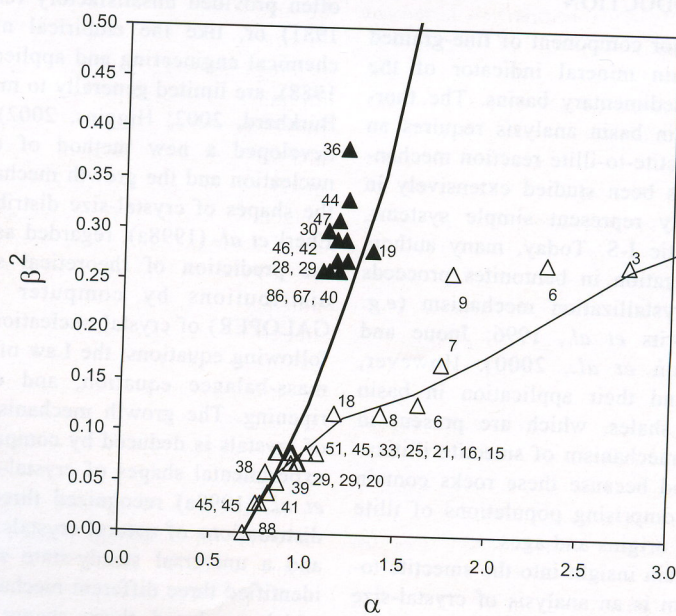


Figure 1. Position of the bentonite samples (open triangles) of Środoń *et al.* (2000), used for reference and the positions of the investigated shale samples (filled triangles) on the plot of Eberl *et al.* (1998a). The plot shows the theoretical paths of evolution of crystal-size distributions for different crystal growth mechanisms; thick line – continuous nucleation and growth; thin line – surface-controlled open-system growth. The numbers by the sample plots represent values of %S obtained from XRD measurements. Note that for bentonites there is a relationship between the %S values and the sample positions in the  $\alpha$  vs.  $\beta^2$  space: generally, the less smectite, the larger  $\alpha$  and  $\beta^2$ . The lack of a similar trend for shales indicates the heterogeneous origin of the asymptotic distributions in those rocks.

of illite crystal (T) of 3 nm, and then turns

The present above findings samples come SE Poland. The thickness distribution of illite (2002) presents measuring the X-ray dif Averbach (BV electron micro treated, <0.2  $\mu$  (Eberl *et al.*, technique (Mu with modeling crystal thickness measurements. I of XRD-determined interpreted in illitization in sha the geology of th the measurement used, refer to Du

CRYST

Illite crystal- XRD for the st (frequencies nor experimental distrib lognormal distrib tion 1, using  $\alpha$  and experimental data of the distributions the Figure (see also samples are arranged of illitization. Sar (Figure 2b) come onset of illitization Dudek, 2001).

Figure 2 clearly mental distribution considerably from 2 nm crystals (asym most illitic sample (Figure 2m).

Figure 3 shows number of smectite because XRD does measurements are pr Dudek *et al.* (2002)) tion: smectite monol I-S, their number dec appears (down to a fe

$g(x)$  is defined as  
 $r$ , whose logarithm

$$\left. \begin{array}{l} -\alpha)^2 \\ \beta^2 \end{array} \right\}$$

0 for  $x \leq 0$  (1)

parameters that  
 variance of  $\ln x$ ,

(2)

(3)

frequency of  $x$ , and  $x$

the three-stage  
 on in bentonites  
 tion of 2 nm illite  
 illitization, until I-S  
 is formed (at  
 (2) nucleation of  
 e accompanied by  
 ers are consumed  
 s for  $R = 0$  I-S,  
 e shape of crystal  
 s, the growth of  
 shape of distribu-  
 controlled growth

of illite crystals, which, until at least a mean thickness ( $\bar{T}$ ) of 3 nm, seems to proceed only in the  $c^*$  direction, and then turns into three-dimensional growth.

The present contribution is an attempt to test if the above findings also apply to diagenetic shales. The shale samples come from the Miocene Carpathian Foredeep of SE Poland. This paper is the second part of the study of thickness distributions (dimension along the  $c^*$  direction) of illite crystals. The first paper (Dudek *et al.*, 2002) presents a comparison of two techniques for measuring the thickness distributions of illite crystals, the X-ray diffraction technique of Bertaut-Warren-Averbach (BWA) and high-resolution transmission electron microscopy (HRTEM), both applied to PVP-treated,  $<0.2 \mu\text{m}$  fractions of Na-exchanged samples (Eberl *et al.*, 1998b). It was shown that the XRD technique (MudMaster computer program combined with modeling of illite 001 reflections) gives reliable crystal thickness data, more accurate than the HRTEM measurements. In the present contribution, the same set of XRD-determined crystal-thickness distributions is interpreted in terms of a mechanism of smectite illitization in shales. For the description of the materials, the geology of the study area, the sample preparation and the measurement methods, as well as the terminology used, refer to Dudek *et al.* (2002).

#### CRYSTAL-THICKNESS DATA

Illite crystal-thickness distributions measured by XRD for the studied shales are shown in Figure 2 (frequencies normalized to 1). In each case, the experimental distribution is compared to the theoretical lognormal distribution calculated according to equation 1, using  $\alpha$  and  $\beta^2$  parameters calculated from the experimental data (equations 2 and 3). The parameters of the distributions of the studied samples are shown in the Figure (see also Table 5 in Dudek *et al.*, 2002). The samples are arranged according to the increasing degree of illitization. Samples RW-1 (Figure 2a) and Z12-6 (Figure 2b) come from the parts of profiles above the onset of illitization, as detected by XRD (Figure 4.6 in Dudek, 2001).

Figure 2 clearly shows that in shales, the experimental distributions of illite crystal thickness deviate considerably from lognormality, due to a large excess of 2 nm crystals (asymptotic-type distribution). Only in the most illitic sample is the deviation reduced noticeably (Figure 2m).

Figure 3 shows that in shales, as in bentonites, the number of smectite monolayers (HRTEM data used here because XRD does not detect monolayers – HRTEM measurements are precise for thin crystals, as shown by Dudek *et al.* (2002)) decreases with progressing illitization: smectite monolayers are most abundant in  $R = 0$  I-S, their number decreasing considerably when ordering

this study, in Figures 1, 3, 4 and 5, the distributions of illite crystal thickness are compared with a set of Pt-shadowing TEM data for bentonites (Środoń *et al.*, 2000). The microscopic methods of measurement of crystal thickness are assumed to be reliable for samples containing thin crystals and characterized by narrow distributions. This is the case for the selected set of bentonites.

#### INTERPRETATION AND DISCUSSION

##### *The origin of asymptotic-type illite-thickness distributions in shales*

Eberl *et al.* (1998a) interpreted the asymptotic-type distributions of crystal size in open systems as an effect of a unique mechanism: simultaneous nucleation and growth of 2 nm crystals with constant or accelerating nucleation rate. Kile *et al.* (2000) experimentally produced an asymptotic-type distribution of calcite crystals (average size from 2.6 to 8.9 nm) by continuous addition of reactants to the solution that was supersaturated with respect to calcite. This led to the continuous nucleation and growth of calcite crystals, providing experimental verification of the validity of the Eberl *et al.* (1998a) model. The illite crystal-thickness distributions of the studied shales are presented in Figure 1. They plot close to the theoretical line, which corresponds to the above mechanism. The interpretation of this trend in terms of the reaction mechanism would be justified if the samples were authigenic (products of *in situ* reaction). However, illite crystals in shales are heterogeneous assemblages resulting from sedimentary mixing of detrital material coming from various source rocks and, above maximum paleotemperatures  $>>70^\circ\text{C}$ , also of superposed diagenetic modification of this material. The mixed nature of the illitic fraction of diagenetic shales has been confirmed by K-Ar dating of the finest separable size-fraction ( $<0.02 \mu\text{m}$ ) (Clauer *et al.*, 1997). The diverse origins for the illite crystals do not permit an interpretation of the mechanism of smectite illitization in shales from the diagenetic evolution of the shape of the overall illite crystal thickness distributions, as can be done for the bentonitic samples.

We think that the asymptotic-type distribution of thickness of illite crystals in shales is produced by the superposition of at least two populations of illite crystals, those which diffract as mixed-layer I-S and discrete illite. The presence of those two phases is shown in XRD patterns of glycolated samples as two sets of peaks (Figure 2 in Dudek *et al.*, 2002). The asymptotic-type distribution is originally a product of sedimentary mixing, as shown by samples RW-1 and Z12-6, which represent parts of the diagenetic profiles above the onset of illitization. Diagenetic illitization gradually modifies this inherited shape and at the level of  $\sim 20\%S$ , the shape

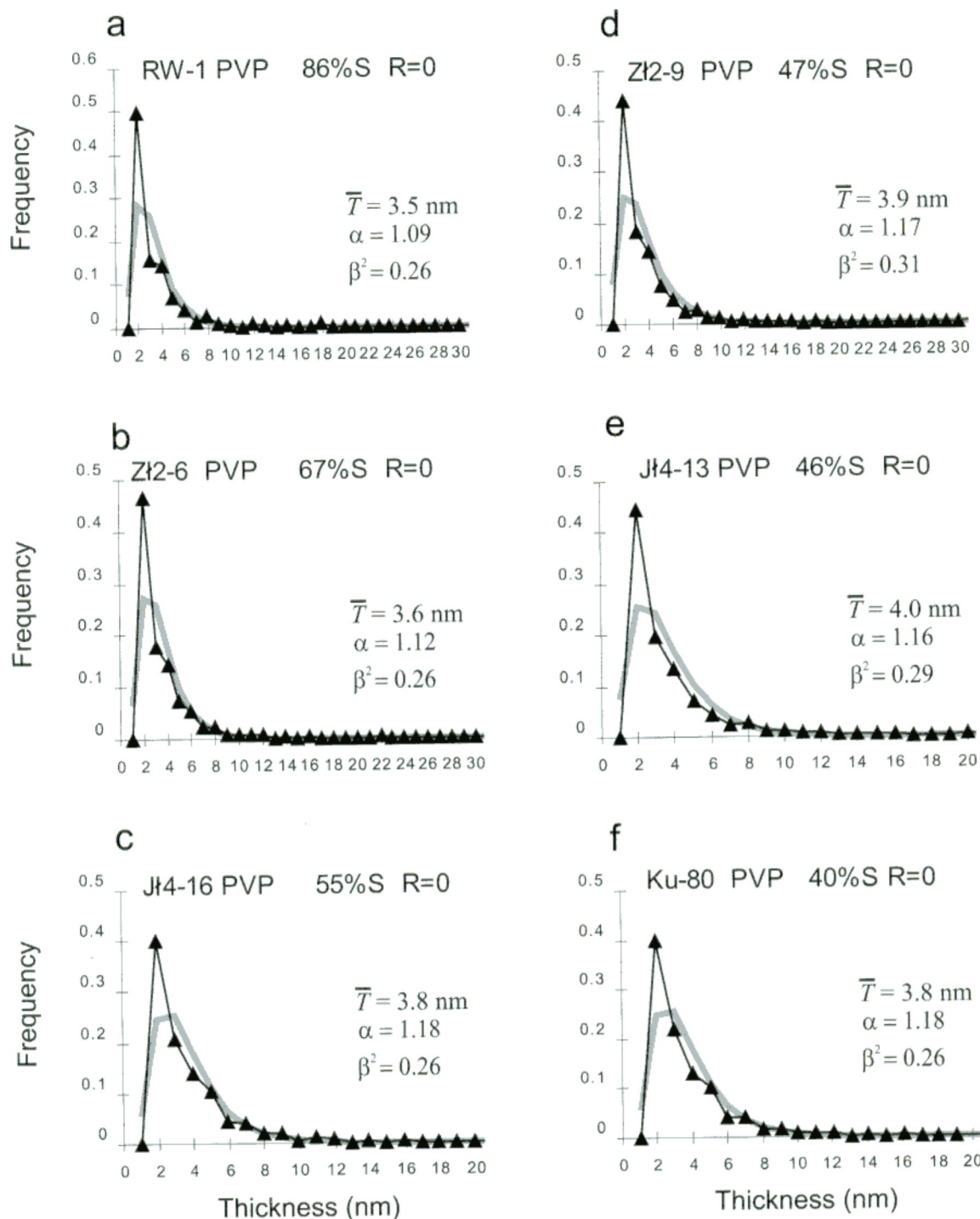


Figure 2. (Above and facing page) Distributions of illite crystal thickness in the studied shales (a–m) measured by the XRD method (MudMaster computer program). Experimental data are marked with triangles; gray lines represent theoretical lognormal distributions calculated from those data using equations 1, 2 and 3. The distribution parameters: mean thickness ( $\bar{T}$ ) in nm,  $\alpha$  and  $\beta^2$  are given for each sample.

discussion that follows, four tests were carried out to verify the suggested origin of the asymptotic-type distributions in shales.

$\%S$  vs. sample position in the  $\alpha$  vs.  $\beta^2$  space. In Figure 1, plots of shale samples are identified by the numbers indicating the degree of smectite illitization (%S,

R=0

3.9 nm  
= 1.17  
= 0.31

2 24 26 28 30

R=0

$\bar{T} = 4.0$  nm  
 $\alpha = 1.16$   
 $\beta^2 = 0.29$

4 16 18 20

S R=0

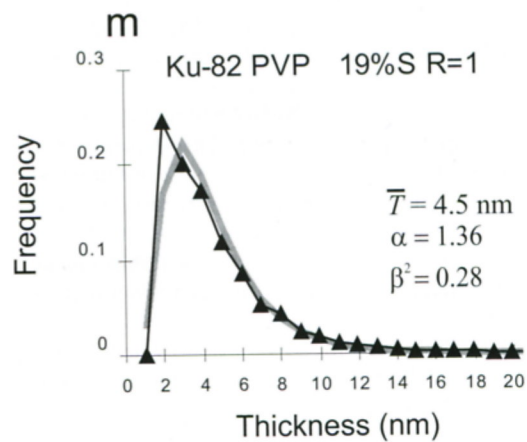
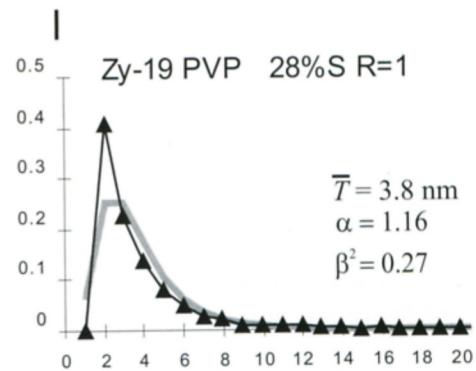
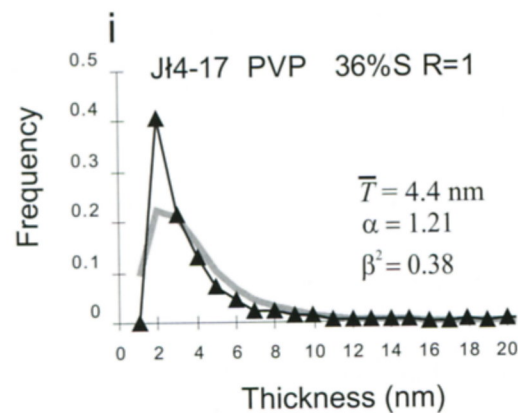
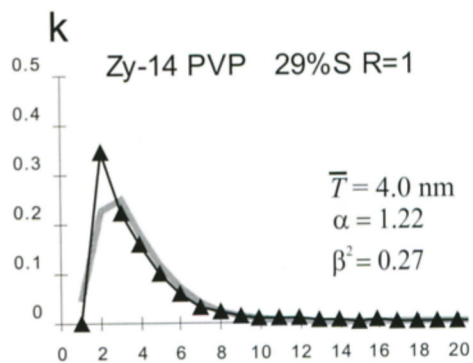
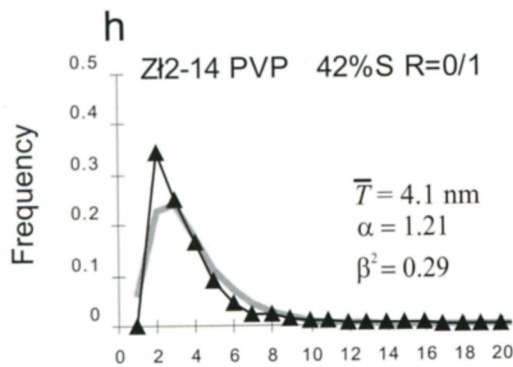
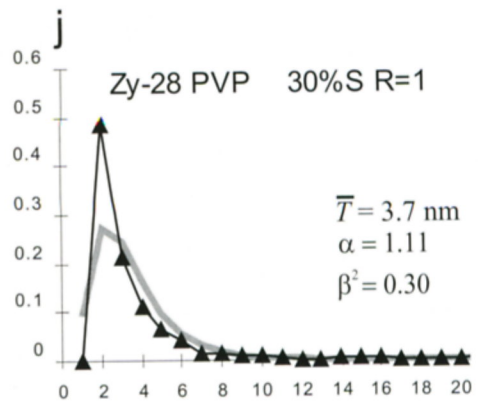
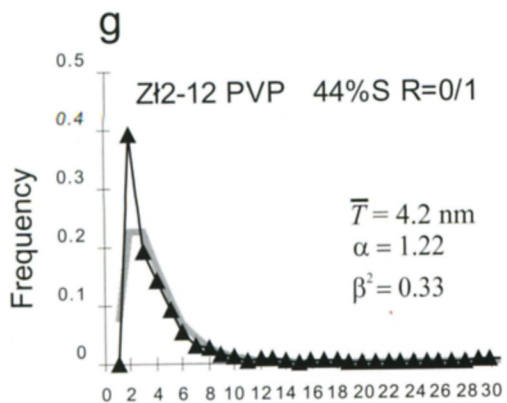
$\bar{T} = 3.8$  nm  
 $\alpha = 1.18$   
 $\beta^2 = 0.26$

14 16 18 20

(nm)

d by the XRD method  
theoretical lognormal  
ness ( $\bar{T}$ ) in nm,  $\alpha$  and  $\beta^2$

space. In Figure 1,  
ed by the numbers



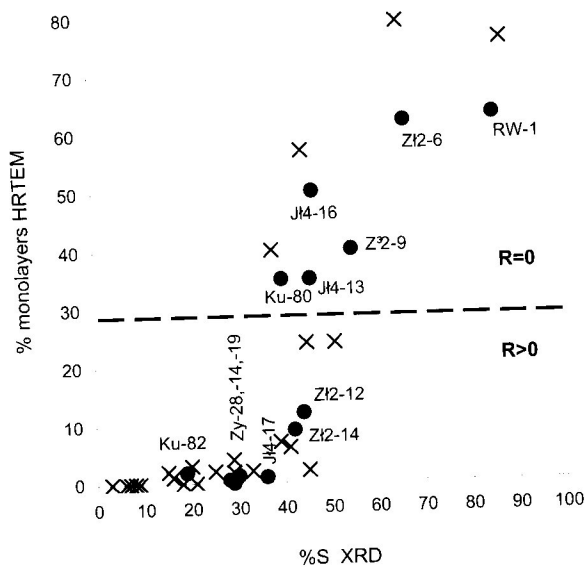


Figure 3. A plot showing the decreasing number of smectite monolayers (HRTEM measurements) in the studied shales (black spots) with increasing degree of diagenesis (expressed as expandability, %S, measured by XRD). The data for bentonites studied by Środoń *et al.* (2000) are plotted for comparison (x). The dashed line separates  $R = 0$  from  $R > 0$  samples.

measured by XRD). The same is shown for a set of bentonites from Środoń *et al.* (2000). A relationship between %S values and the sample positions in the  $\alpha$  vs.  $\beta^2$  space, like that observed for bentonites (generally, the smaller %S, the bigger  $\alpha$  and  $\beta^2$ ), would have been expected if the samples were composed of a single population of crystals related by a unique growth mechanism. The lack of such correlation for shales confirms the heterogeneous origin of the asymptotic distributions in those rocks.

*Relationship between distributions of illite crystals in shales and bentonites.* The purpose of this test is to compare the distributions of thickness of illite crystals in the studied shale samples with the distributions in the reference bentonitic samples, which represent a similar stage of diagenetic evolution of I-S. The measurements of bentonites (Środoń *et al.*, 2000) were used to match the shale samples. The criterion for selecting the proper bentonite (or bentonites) to compare with the shale was similar %S values and ordering. The comparison is presented in Figure 4(a–m), where the samples are arranged according to the increasing degree of illitization. The following observations can be made:

(1) Each shale sample contains fewer thin crystals and considerably more thick crystals compared with the corresponding bentonitic sample.

(2) The shale distributions are polymodal. Two populations of illite crystals can be distinguished in the 2–12 nm thickness range in shales: (a) very thin illite (with a maximum at the 2 nm category) which corre-

sponds to the illite crystals forming mixed-layer crystals in bentonites; and (b) thicker illite (with maximum at 3–5 nm), which produces a ‘tail’ of crystals outside the distribution characteristic of bentonites. The two populations are clearly visible in samples less evolved diagenetically, characterized by smaller mean thicknesses (Figure 4a–e).

(3) The thickness of illite crystals within the finer population increases progressively during illitization; the thickness of illite crystals in the coarser population does not show a visible trend.

Shale and bentonitic samples in each case are characterized by a similar degree of smectite illitization, thus it can be expected that the population of very thin illite in shales, which corresponds to the distribution of illite crystals in bentonites, account for I-S interstratifications. The remaining crystals represent discrete illite and coarser mica. However, crystals as thin as 2 nm can also contribute to the population of discrete illite, as is clearly seen in Figure 4a,b. This issue will be considered below in more detail.

*The thickness of illite crystals forming I-S vs. discrete illite.* The coexistence of illite crystals that form I-S interstratifications and those that produce a discrete 10 Å peak in the shale samples can also be shown by comparison of %S values obtained in two different ways: (1) directly from the XRD patterns of the glycolated samples (%S<sub>XRD</sub>) using the techniques of Środoń (1981, 1984), and (2) by using the values of mean thickness ( $\bar{T}$  in nm) of illite and smectite crystals to calculate %S<sub>MAX</sub>, where %S<sub>MAX</sub> = 100/ $\bar{T}$  (Środoń *et al.*, 1992). Again, the bentonites of Środoń *et al.* (2000) were taken for reference. If all (or the majority of) illite crystals in shales formed a single population accounting for I-S mixed-layers (as in bentonites), the relationship between the two values of %S for shales would be the same as for bentonites.

This test is based on the observations of Środoń *et al.* (1992) that for bentonites, %S<sub>MAX</sub> is always larger than %S<sub>XRD</sub>. This discrepancy was explained as a result of the restricted size of mixed-layer crystals: in XRD patterns of I-S, only smectite interlayers within mixed-layer crystals are accounted for, while the %S<sub>MAX</sub> calculation also takes into account the tops and bottoms of mixed-layer crystals. The %S<sub>MAX</sub> calculations of Środoń *et al.* (1992) were based on Pt-shadowing TEM measurements of  $\bar{T}$  of I-S fundamental particles (the calculation requires inclusion of smectite monolayers). Here %S<sub>MAX</sub> is calculated using  $\bar{T}$  values estimated by the XRD-BWA method, because it was shown that these values are more precise than  $\bar{T}$  obtained using the HRTEM technique (Dudek *et al.*, 2002). Therefore, not all shale samples but only those devoid of smectite monolayers were taken into account in this test.

Figure 5 shows that for shales, the relationship between %S<sub>MAX</sub> and %S<sub>XRD</sub> is different from that for

bentonites: %S<sub>MAX</sub> evidence that in shales (discrete illite, mixed-layer interstratifications) refers only to mixed-layer does not differentiate to interparticle discrete illite. %S<sub>MAX</sub> represents illite component in I-S mixed-layer.

Going a step further, estimate of the overlap with the amount of discrete illite calculate %S<sub>MAX</sub>. This was done by (i.e. by limiting at the maximum that although the direction (i.e. to even the elimination 5 nm does not trends. These fraction of shale (assuming that size as those in observations from

In the literature the thickness of discrete 10 Å particles (Środoń *et al.* (1985) and shadowing TEM composed of smectite I-S or discrete illite produced a mixed-layer regarded as I-S effect, pure illite showed the distribution of crystals 2–12 nm (2000) identified characterized by lognormal distribution evidence of interparticle were characterized were virtually

Uhlik *et al.* method the thickness of clay fraction in the East Slova used in this study %S<sub>XRD</sub>), they contains a new the relationship samples devoid suite of bentonite

ixed-layer crystals  
with maximum at  
crystals outside the  
es. The two popu-  
ples less evolved  
aller mean thick-  
s within the finer  
during illitization;  
coarser population

in each case are  
smectite illitization,  
lation of very thin  
the distribution of  
for I-S interstrati-  
esent discrete illite  
as thin as 2 nm can  
discrete illite, as is  
will be considered

ng I-S vs. discrete  
tals that form I-S  
roduce a discrete  
also be shown by  
two different ways:  
of the glycolated  
es of Środoń (1981,  
mean thickness ( $\bar{T}$ )  
o calculate %S<sub>MAX</sub>,  
, 1992). Again, the  
e were taken for  
illite crystals in  
accounting for I-S  
relationship between  
d be the same as for

ons of Środoń *et al.*  
always larger than  
ained as a result of  
crystals: in XRD  
ayers within mixed-  
while the %S<sub>MAX</sub>  
e tops and bottoms  
AX calculations of  
Pt-shadowing TEM  
ental particles (the  
ectite monolayers).  
values estimated by  
as shown that these  
obtained using the  
002). Therefore, not  
devoid of smectite  
in this test.  
s, the relationship

bentonites: %S<sub>MAX</sub> is usually <%S<sub>XRD</sub>. This is the evidence that in shales there is a fraction of illite crystals (discrete illite, mica) other than those contributing to I-S interstratifications. Expandability measurement by XRD refers only to mixed-layer crystals. In contrast, %S<sub>MAX</sub> does not differentiate between illite crystals contributing to interparticle diffraction, and those diffracting as discrete illite. Consequently,  $\bar{T}$  used for calculating %S<sub>MAX</sub> represents the sample as a whole. The discrete illite component must, on average, be thicker than illite in I-S mixed-layers, because %S<sub>XRD</sub> > %S<sub>MAX</sub>.

Going a step further, in order to make a rough estimate of the extent to which discrete illite crystals overlap with those which contribute to I-S interstratifications, an attempt was made to 'eliminate' a certain amount of discrete illite from the samples and to calculate %S<sub>MAX</sub> using  $\bar{T}$  of these reduced distributions. This was done by cutting off a number of thick crystals (*i.e.* by limiting the distributions at the coarse end) first at the maximum of 10 nm, then at 5 nm. Figure 5 shows that although the trend for shales shifts in the expected direction (*i.e.* towards the trend formed by bentonites), even the elimination of all illite crystals thicker than 5 nm does not produce a satisfying overlap of the two trends. These results indicate that the  $\leq 5$  nm illitic fraction of shales contains discrete illite crystals (assuming that I-S crystals in shales are of the same size as those in bentonites), which is consistent with the observations from Figure 4.

In the literature, there are contrasting observations on the thickness distribution of illite crystals that produce discrete 10 Å peaks in XRD diffraction patterns. Nadeau *et al.* (1985) and Środoń *et al.* (2000), using the Pt-shadowing TEM technique, investigated illitic samples composed of single populations of illite crystals (either I-S or discrete illite, *i.e.* when interparticle diffraction produced a mixed-layering effect, the sample was regarded as I-S, whereas with no interparticle diffraction effect, pure illite was identified). Nadeau *et al.* (1985) showed the distributions of discrete illite, which consist of crystals 2–17 nm thick (mean 5 nm). Środoń *et al.* (2000) identified 3–9% of expandable layers in samples characterized by the mean thickness of ~5–6 nm and a lognormal distribution. Pure illites with no XRD evidence of interparticle diffraction (Kamikita samples) were characterized by mean thicknesses >10 nm and were virtually devoid of 2 nm crystals.

Uhlik *et al.* (2000) investigated by the PVP-HRTEM method the thickness distribution of illite crystals in the clay fraction of four diagenetically altered shales from the East Slovak Basin. Applying the same approach as used in this study (*i.e.* the comparison of %S<sub>MAX</sub> and %S<sub>XRD</sub>), they deduced that the  $\leq 10$  nm illitic fraction contains a negligible amount of discrete illite, because the relationship between %S<sub>XRD</sub> and %S<sub>MAX</sub> for their samples devoid of  $\geq 10$  nm crystals was similar to the

discrete illite crystals were found to be generally >10 nm. Uhlik *et al.* (2000) concluded that the PVP-HRTEM technique could be used to determine the relative amounts of detrital (discrete) illite vs. authigenic illite in shale samples.

Data contradictory to those of Uhlik *et al.* (2000) were reported by Elsass *et al.* (1997) on the basis of the HRTEM studies. In the Pennsylvanian underclay they detected discrete illite dominated by 2 nm thick crystals in a mixture with I-S.

The results of the present study support the observations of Nadeau *et al.* (1985) and Elsass *et al.* (1997) that very thin crystals can diffract as discrete illite.

#### *Asymptotic distribution as a mixture of lognormal distributions*

It can be shown by modeling that an asymptotic shape can be generated by superposition of a number of lognormal distributions, which serves as a model of mixing clays of different origins. We used lognormal distributions, because they are characteristic of the populations of illite crystals in bentonites resulting from a single crystallization event (Środoń *et al.*, 2000), and therefore can be regarded as original distributions of the components of a mixture. This is only an approximation, because at present, we do not know the effects of weathering and transportation processes on the shape of thickness distribution of illite crystals. It will be shown below that even such approximate modeling reveals interesting information about the evolution of illite crystals in the course of diagenesis.

An example of modeling is shown in Figure 6. The shape of illite crystal-thickness distribution of sample J14-17 was simulated using the smallest possible number of lognormal distributions with  $\alpha$  vs.  $\beta^2$  typical of bentonites (Eberl *et al.*, 1998a, Figure 12). The best fit was obtained if three lognormal distributions with  $\bar{T}$  equal to 2.2 nm, 5 nm and 20 nm were mixed in proportions 0.33, 0.45 and 0.22, respectively (mass frequencies were used, see below). The modeling agrees well with the heterogeneous nature of illite crystal populations in shales: to model the experimental distributions, at least three lognormal shapes are needed.

All described computational experiments confirm the complex nature of illite crystal-thickness distributions in diagenetic shales. Thus, unless independent data (*e.g.* K-Ar dating) indicate that the studied fraction of crystals can be regarded as diagenetic, extreme caution should be exercised when interpreting illite crystal-thickness distributions in terms of the smectite illitization mechanism in shales. Therefore we believe that the conclusions of Brime *et al.* (2002) and Brime and Eberl (2002) who determined the nucleation and growth paths on the  $\alpha$  vs.  $\beta^2$  plot for their low-grade illites from shales using the

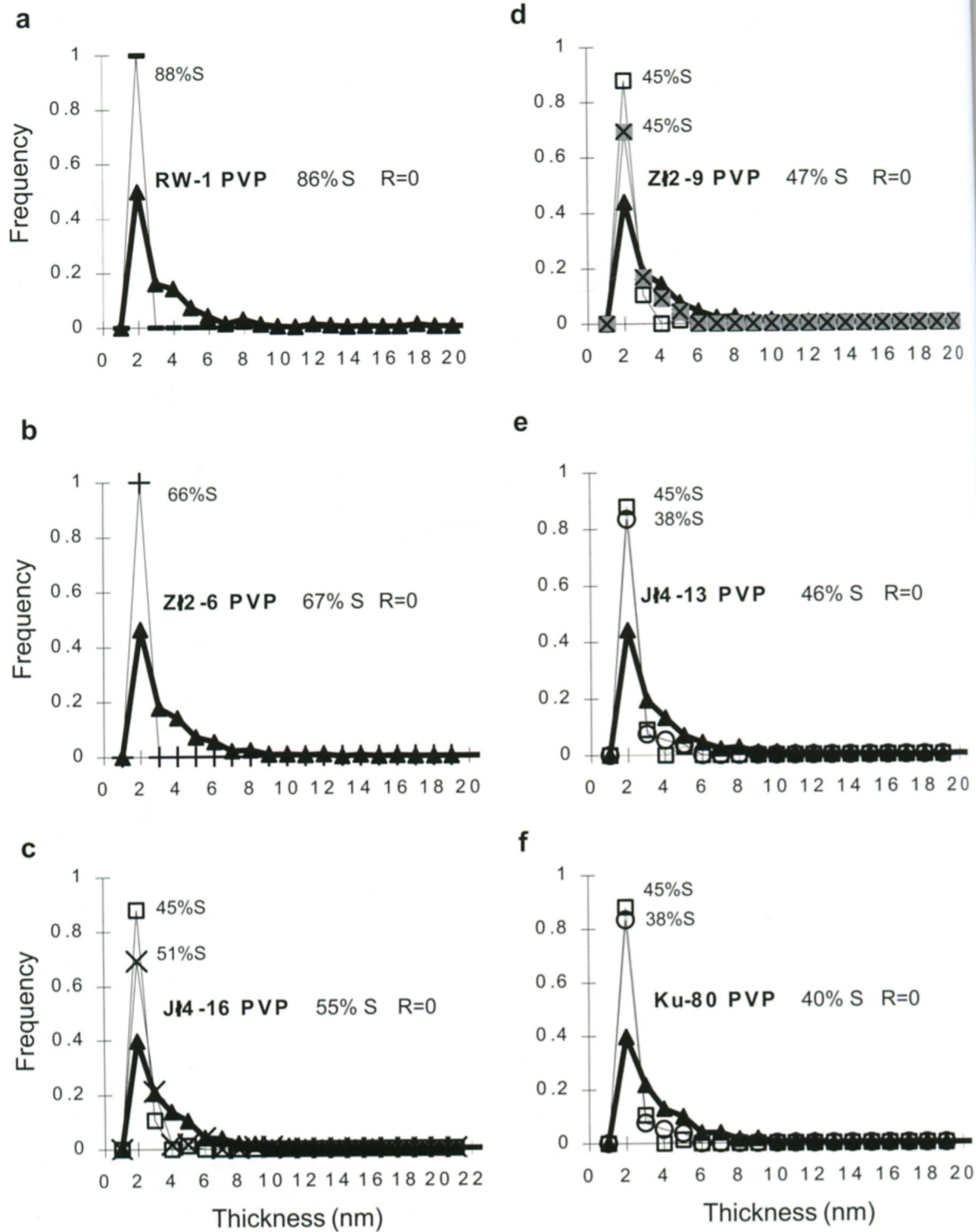
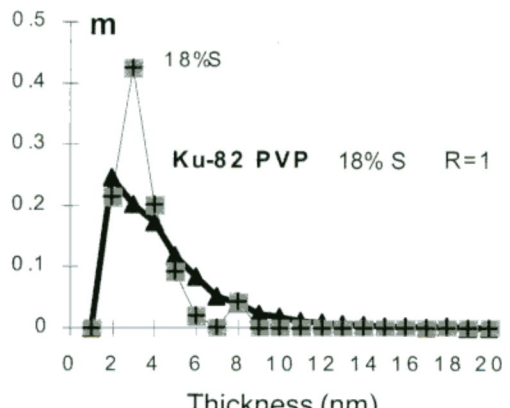
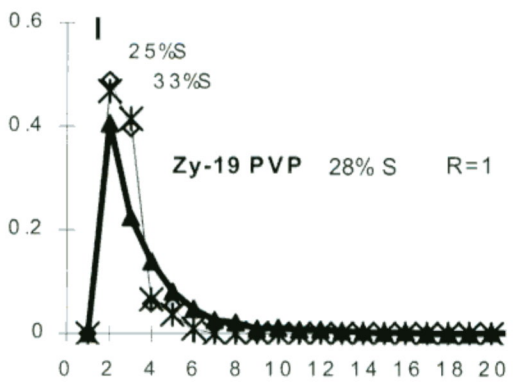
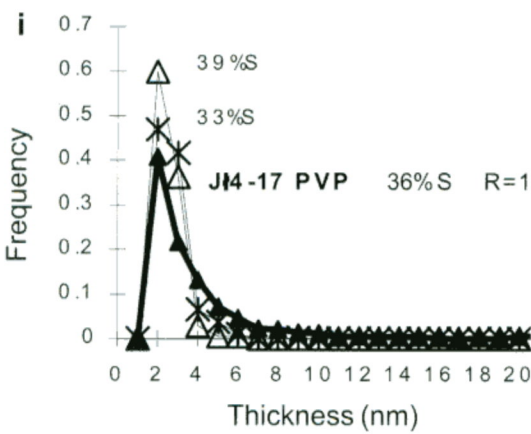
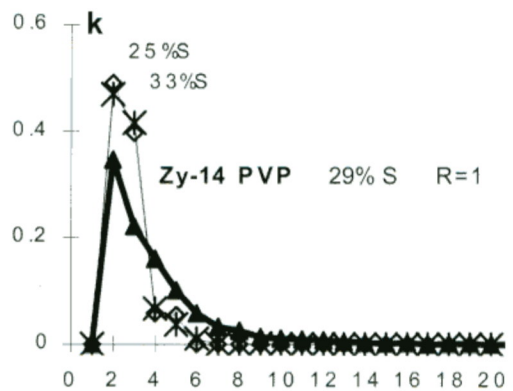
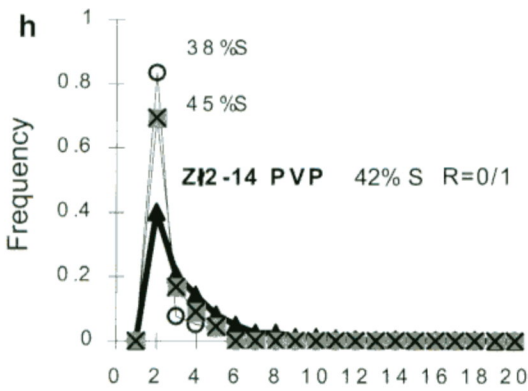
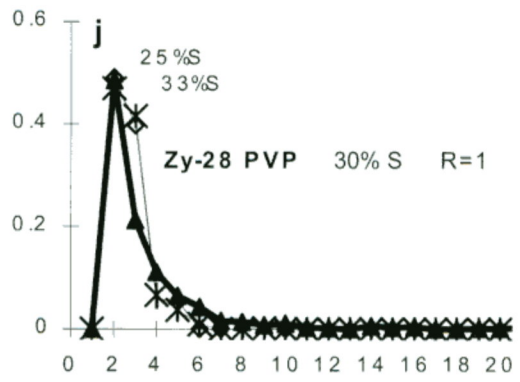
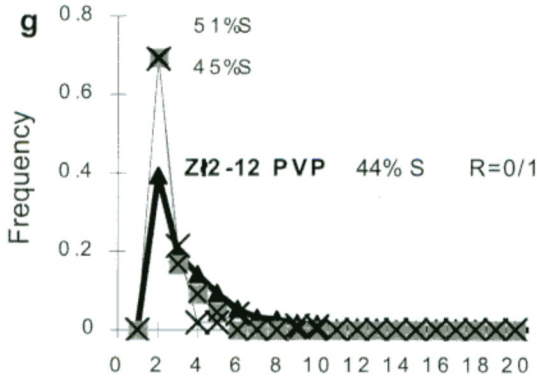


Figure 4. (Above and facing page) Comparison of illite particle thickness distributions in the studied shales (XRD data, thick line) with the distributions in bentonites (Pt-shadowing TEM measurements of Środoń *et al.*, 2000, area-weighted thickness distributions, thin lines). Samples of shales and bentonites in each case are characterized by a similar degree of smectite illitization (%S measured by XRD and ordering). In most cases, more than one bentonitic sample is used.





% S R=0

14 16 18 20

% S R=0

14 16 18 20

% S R=0

14 16 18 20

(nm)

(XRD data, thick line)  
thickness distributions,  
ization (%S measured)

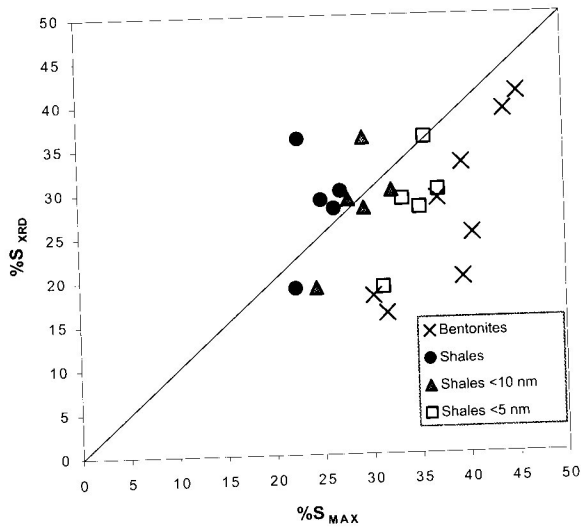


Figure 5. Comparison of expandabilities of the studied shales determined from the diffraction patterns ( $\%S_{XRD}$ ) and calculated from the mean thickness of fundamental particles ( $\%S_{MAX}$ ). The data for bentonites (Środoń *et al.*, 2000) are used for reference. Displacement of shale plots (dots) with respect to bentonite plots (x) towards smaller  $\%S_{MAX}$  is taken as evidence of the contribution of discrete illite crystals, on average thicker than those forming mixed-layer crystals, but also containing crystals <5 nm (see text for details).

*Mechanism of smectite illitization in shales inferred from direct examination of illite crystal-thickness distributions*

To be able to study the mechanism of smectite illitization in the investigated shales, an attempt was made to trace the relative gains and losses of crystals of different thickness during diagenesis. To do this, the distributions must be normalized to a constant mass. Thus two conditions must be fulfilled: (1) all crystals in the samples should be accounted for, *i.e.* the distributions should include smectite monolayers; and (2) mass frequencies of crystal thickness classes should be used instead of number frequencies. Monolayers were included

in the illite thickness distributions determined by XRD by using the HRTEM-measured proportions of monolayers and 2 nm crystals. Mass frequencies were calculated by multiplying number frequency by crystal thickness for each thickness class.

We showed that at least three lognormal distributions should be used to model asymptotic-type distributions in shales (Figure 6). In order to be able to trace the relative gains and losses of the crystal classes in shales during diagenesis, we had to establish a set of reference lognormal distributions and use them to model the experimental asymptotic-type distributions in shales. The mean thicknesses of the reference lognormal distributions are as follows: 1 nm, 1.5 nm, 2 nm, 3 nm, 4 nm, 4.5 nm, 5.5 nm, 14.2 nm and 20 nm. The distributions from 1 nm to 5.5 nm represent a continuous sequence. A gap between 5.5 nm, 14.2 nm and 20 nm reference distributions results from the shape of experimental distributions: starting from 7–8 nm thickness class, the frequencies usually fall below 0.05. To model this tail of thick crystals one or two distributions are sufficient. The best fit was obtained by trial and error using the smallest possible number of reference lognormal distributions. It is worth re-emphasizing again that the presented decomposition of distributions in shales does not have precise physical meaning, *i.e.* the studied samples are not necessarily composed of the selected set of lognormal distributions. However, this exercise is a good tool to show uniform general trends of diagenetic evolution of the overall illite crystal-thickness distributions during shale diagenesis.

The results of the exercise are shown in Figure 7, where the samples are arranged according to the increasing degree of smectite illitization. Distributions of the two purely detrital samples (RW-1 and Z12-6) have clear gaps: curves representing  $\bar{T} = 2$  nm and  $\bar{T} = 3$  nm are not needed in the model. We assume that the portion below  $\bar{T} = 4$  nm (left of the black line) represents I-S (~40% of the mass) and the coarser portion (right of the black line) accounts for the discrete

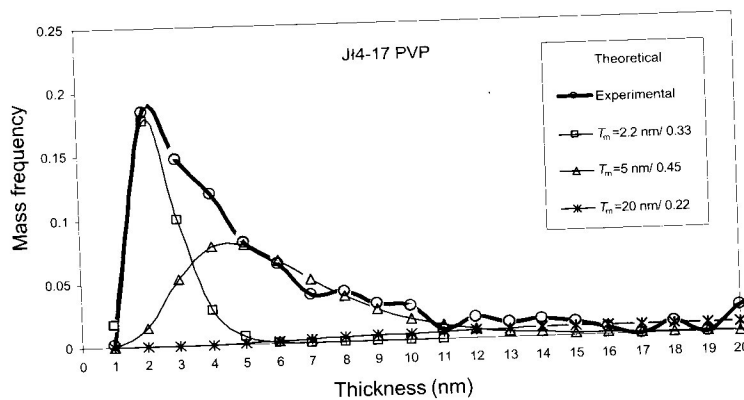


Figure 6. Modeling of the asymptotic-type distribution of the sample J14-17 by superposition of the smallest possible number of theoretical lognormal distributions characterized by <5 nm equal to 2.2 nm, 5 nm and 20 nm mixed in proportions 0.33, 0.45 and 0.22, respectively.

Detrital Diagenetic

Figure 7. Modelled possible number of 3 nm, 4 nm, 4.5 nm discrete illite. The

illite. Proportion from sample to is no clear demonstrates illite crystal diagenesis. T distributions r dashed gray line (between the c illite compone analysis confi the distributio analysis appea discrete illite

An alterna the overall d fraction of ill tions and to results of this we decided convey intere

The two s depths above

etermined by XRD  
portions of mono-  
frequencies were  
quency by crystal

ormal distributions  
pe distributions in  
o trace the relative  
s in shales during  
set of reference  
em to model the  
utions in shales.  
erence lognormal  
5 nm, 2 nm, 3 nm,  
1 20 nm. The dis-  
esent a continuous  
4.2 nm and 20 nm  
e shape of experi-  
7–8 nm thickness  
ow 0.05. To model  
o distributions are  
by trial and error  
f reference lognor-  
hasizing again that  
tributions in shales  
ing, *i.e.* the studied  
d of the selected set  
t, this exercise is a  
rends of diagenetic  
l-thickness distribu-

shown in Figure 7,  
according to the  
ation. Distributions  
(RW-1 and Z12-6)  
g  $\bar{T} = 2$  nm and  $\bar{T} =$   
We assume that the  
of the black line)  
(s) and the coarser  
ounts for the discrete

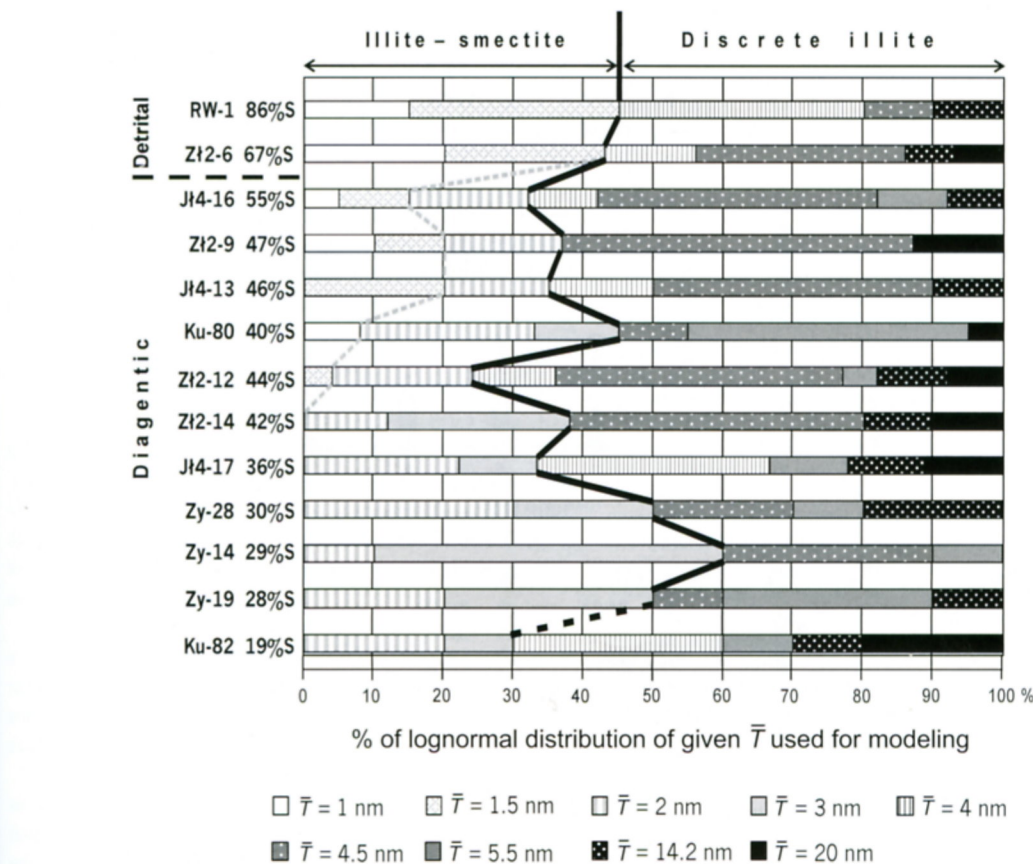


Figure 7. Modeling of asymptotic distributions of illite crystal thickness for all shale samples by superposition of the smallest possible number of lognormal distributions chosen from a group of nine basic distributions (mean thicknesses of 1 nm, 1.5 nm, 2 nm, 3 nm, 4 nm, 4.5 nm, 5.5 nm, 14.2 nm and 20 nm). The best fit was obtained by trial and error. The black line separates fields of I-S and discrete illite. The gray line illustrates the diagenetic evolution of I-S. See text for details.

illite. Proportions between the two components fluctuate from sample to sample (from 20 to 60% of I-S), but there is no clear trend related to diagenesis. Figure 7 demonstrates clearly that the two components of the illite crystal distribution behave differently during diagenesis. The I-S component evolves gradually: distributions representing fine  $\bar{T}$  decrease (left of the dashed gray line), and distributions with bigger  $\bar{T}$  appear (between the dashed gray and black lines). The discrete illite component does not show any clear trend. Our analysis confirms the observations made by inspecting the distributions presented in Figures 2 and 4. The analysis appears to offer a method of quantifying I-S vs. discrete illite in the illitic fraction of shales.

An alternative attempt was also made to extract from the overall distributions of the investigated shales the fraction of illite crystals that produce I-S interstratifications and to trace its evolution during diagenesis. The results of this exercise are very approximate. However, we decided to present them, because they seem to convey interesting information.

The two samples (RW-1 and Z12-6) that come from depths above the onset of illitization, hereafter referred

to as 'detrital samples', were used again as starting points. The overall distributions of RW-1 and Z12-6 samples were split into I-S and discrete illite fractions by using for reference the bentonite samples 2M9 and M3, respectively, characterized by similar proportions of illite to smectite layers in I-S, as measured by XRD (data of Środoń *et al.*, 2000). Assuming that all monolayers in the shale samples participate in I-S interstratification, the fraction of 2 nm crystals belonging to I-S was adjusted so that the proportion between monolayers and 2 nm crystals in the shale I-S was the same as in the bentonite I-S (no 3 nm crystals in the bentonitic samples). Subtracting all smectite and adjusting the fraction of 2 nm crystals, the crystal-thickness distributions of discrete illite were obtained. Illite crystals producing I-S interstratifications in the remaining shale samples, representing the rocks that have passed into the burial diagenesis zone (hereafter referred to as 'diagenetic samples'), were extracted by subtracting these distributions of discrete illite obtained from the detrital samples. The fraction of the subtracted distribution was kept constant for all samples. This approach requires an assumption that discrete illite does not change during

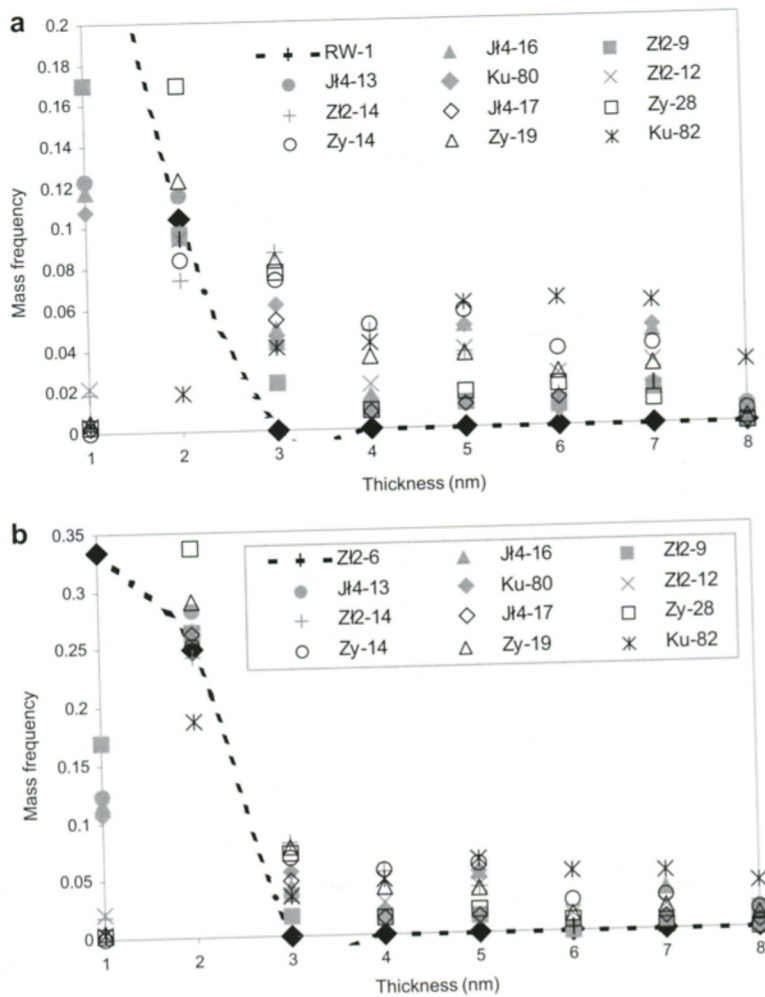


Figure 8. Thickness distributions of illite crystals contributing to I-S interstratifications in the studied shales, extracted from overall distributions by subtracting the fraction of discrete illite crystals. The distributions of discrete illite crystals were obtained for two detrital samples, RW-1 (a) and ZI2-6 (b), using the distributions of reference bentonitic samples 2M9 and M3, respectively, to remove the I-S contributions (see text for details). The samples in the legend are arranged according to increasing degree of illitization. Detrital samples: filled black diamonds, diagenetic samples: filled gray symbols ( $R = 0$  interstratification), open black symbols ( $R > 0$  interstratifications). The figures show that during illitization the proportion of smectite monolayers decreases, the proportion of 2 nm thick illite crystals changes inconspicuously compared to the detrital samples, and the biggest gain of mass of I-S is due to crystals equal to, and greater than, 3 nm. This implies that the principal mechanism of smectite illitization in shales is the growth of 2 nm thick illite crystals.

diagenesis, which, at least in the clay fraction of the studied section, seems acceptable (see Figure 7). However, sedimentary variation of the discrete illite fraction (Figure 7) is not accounted for by this approach.

The results of this exercise are presented for RW-1 (Figure 8a) and for ZI2-6 (Figure 8b) used as the reference detrital samples. The samples in the legend are arranged according to the increasing degree of smectite illitization. In both cases, it can be seen that with progressing illitization, the biggest gain of mass in I-S is due to crystals equal to and thicker than 3 nm. The fraction of 2 nm crystals in the diagenetic samples is either similar to or decreases compared to the detrital samples (sample Zy-28 is an exception). The proportion

of smectite monolayers drops noticeably during diagenesis. Figure 8 indicates that diagenetic illitization of smectite in shales does not involve a massive nucleation of 2 nm thick crystals, but rather the growth of the detrital 2 nm illite crystals at the expense of dissolving smectite monolayers. It seems that the presence of sufficient amounts of detrital 2 nm thick crystals in shales reduces or eliminates the stage of their nucleation (characteristic of bentonites). Such growth may lead to the observed (Šucha *et al.*, 1993) acceleration of smectite illitization in shales with respect to bentonites. However, this model is based on very limited data. It would be too far-reaching a conclusion to suggest it as a general model of smectite illitization in shales. This

mechanism seems reasonable because the detrital illite crystals in all crystals in the situation where detrital smectite monolayers there are only a few to reduce the level of an extreme case), diagenetic illite crystals analogous to that described by Šucha *et al.*, 2000), should be

(1) The asymptotic distributions identified in the studied shales can be interpreted as an effect of illite crystals, discrete illite. Modeling of lognormal distributions with asymptotic distributions (2) The modeling of a number of lognormal distributions for identifying and characterizing components in shale evolution.

(3) The modeling of smectite illitization in shales evolves gradually whereas the discrete illite shows any clear trend.

(4) Being mixed distributions of unillitized data cannot be identified as illitization mechanism (growth) using the discrete illite model of the I-S portion. This indicates the mechanism of the studied shales. Modeling was not observed. The illitization seems to be concentrated in crystals at the edge layers.

This paper received funding from the Polish Academy of Sciences, directed by Dennis D. Eberl, and the quality of the manuscript was improved by the comments of Brime and Jinwoon. The authors thank McCarty for his contribution.

Brime, C. and Eberl, D. D. (1999) High grade illites in bentonites. *Schwartz Petrographica* 1, 1-10.

Brime, C., Castro

mechanism seems reasonable for the studied profile, because the detrital 2 nm crystals account for >16% of all crystals in the detrital samples. However, in a situation where detrital material is dominated by smectite monolayers (very high expandability), and there are only a few 2 nm crystals to grow and thereby to reduce the level of supersaturation (pure bentonite is an extreme case), diagenetic nucleation of 2 nm crystals, analogous to that documented for bentonites (Środoń *et al.*, 2000), should be expected to operate.

### CONCLUSIONS

(1) The asymptotic-type illite crystal-thickness distributions identified in the investigated shales are interpreted as an effect of superposition of populations of illite crystals, forming I-S interstratifications and discrete illite. Modeling shows that a minimum of three lognormal distributions is required to fit the measured asymptotic distributions.

(2) The modeling of asymptotic distributions by using a number of lognormal distributions offers a method of identifying and quantifying I-S and discrete illite components in shales, and tracing their diagenetic evolution.

(3) The modeling shows that with progressive smectite illitization, the I-S component of the distributions evolves gradually towards larger crystal sizes whereas the discrete illite component does not show any clear trend.

(4) Being mixed distributions, in contrast to the distributions of uniform origin in bentonites, bulk shale data cannot be interpreted in terms of the smectite illitization mechanism (simultaneous nucleation and growth) using the approach of Eberl *et al.* (1998b). If the discrete illite component is subtracted, the evolution of the I-S portion of the crystal thickness distributions indicates the mechanism of smectite illitization in the studied shales. Massive nucleation of 2 nm crystals is not observed. The principal mechanism of smectite illitization seems to be the growth of detrital 2 nm illite crystals at the expense of dissolving smectite monolayers.

### ACKNOWLEDGMENTS

This paper reports part of the PhD thesis of Teresa Dudek directed by Jan Środoń. The authors thank Dr Dennis D. Eberl for useful comments and for improving the quality of the English. The reviewers, Covadonga Brime and Jinwook Kim, and the associate editor Douglas McCarty contributed to the clarity of the manuscript.

### REFERENCES

Brime, C. and Eberl, D.D. (2002) Growth mechanism of low-grade illites based on shapes of crystal thickness distributions. *Schweizerisches Mineralogisches und Petrographisches Mitteilungen*, **82**, 203–209.

illitization progress from diagenesis to very low-grade metamorphism in rocks of the Cantabrian Zone (Spain). *Schweizerisches Mineralogisches und Petrographisches Mitteilungen*, **82**, 211–219.

Burkhard, D. (2002) Kinetics of crystallization: example of micro-crystallization in basalt lava. *Contributions to Mineralogy and Petrology*, **142**, 724–737.

Christidis, G.E. (1995) Mechanism of illitization of bentonites in the geothermal field of Milos Island, Greece: Evidence based on mineralogy, chemistry, particle thickness morphology. *Clays and Clay Minerals*, **43**, 569–586.

Clauer, N., Środoń, J., Francù, J. and Šucha, V. (1997) K-Ar dating of illite fundamental particles separated from illite-smectite. *Clay Minerals*, **32**, 181–196.

Drits, V., Salyn, A.L. and Šucha, V. (1996) Structural transformations of interstratified illite/smectites from Dolna Ves hydrothermal deposits: dynamics and mechanisms. *Clays and Clay Minerals*, **44**, 181–190.

Drits, V., Eberl, D.D. and Środoń, J. (1998) XRD measurement of mean thickness, thickness distribution and strain for illite and illite-smectite crystallites by the Bertaut-Warren-Averbach technique. *Clays and Clay Minerals*, **46**, 38–50.

Dudek, T. (2001) Diagenetic evolution of illite-smectite in the Miocene shales from the Przemyśl area (Carpathian Foredeep). PhD thesis, Institute of Geological Sciences, Polish Academy of Sciences, 155 pp.

Dudek, T., Środoń, J., Eberl, D.D., Elsass, F. and Uhlík, P. (2002) Thickness distribution of illite crystals in shales. I: X-ray diffraction vs. high-resolution transmission electron microscopy measurements. *Clays and Clay Minerals*, **50**, 562–577.

Eberl, D.D. and Środoń, J. (1988) Ostwald ripening and interparticle diffraction effects for illite crystals. *American Mineralogist*, **73**, 1335–1345.

Eberl, D.D., Środoń, J., Kralík, M., Taylor, B.E. and Peterman, Z.E. (1990) Ostwald ripening of clays and metamorphic minerals. *Science*, **248**, 474–478.

Eberl, D.D., Drits, V. and Środoń, J. (1998a) Deducing growth mechanisms for minerals from the shapes of crystal size distributions. *American Journal of Science*, **298**, 499–533.

Eberl, D.D., Nuesch, R., Šucha, V. and Tšipursky, S. (1998b) Measurement of fundamental illite particle thicknesses by X-ray diffraction using PVP-10 intercalation. *Clays and Clay Minerals*, **46**, 89–97.

Elsass, F., Środoń, J. and Robert, M. (1997) Illite-smectite alteration and accompanying reactions in a Pennsylvanian underclay studied by TEM. *Clays and Clay Minerals*, **45**, 390–403.

Higgins, M.D. (2002) A crystal-size distribution study of the Kiglapait layered mafic intrusion, Labrador, Canada: evidence for textural coarsening. *Contributions to Mineralogy and Petrology*, **144**, 314–330.

Inoue, A. and Kitagawa, R. (1994) Morphological characteristics of illitic clay minerals from a hydrothermal system. *American Mineralogist*, **79**, 700–711.

Inoue, A., Velde, B., Meunier, A. and Touchard, G. (1988) Mechanism of illite formation during smectite-to-illite conversion in a hydrothermal system. *American Mineralogist*, **73**, 1325–1334.

Kile, D.E., Eberl, D.D., Hoch, A.R. and Reddy, M.M. (2000) An assessment of calcite crystal growth mechanism based on crystal size distributions. *Geochimica et Cosmochimica Acta*, **64**, 2937–2950.

Kirkpatrick, R.J. (1981) Kinetics of crystallization of igneous rocks. Pp. 321–398 in: *Kinetics of Geochemical Processes* (A.C. Lasaga and R.J. Kirkpatrick, editors). Reviews in Mineralogy, **8**. Mineralogical Society of America, Washington, D.C.

- and the kinetics and dynamics of crystallization I. Theory. *Contributions to Mineralogy and Petrology*, **99**, 277–291.
- Nadeau, P.H., Tait, J.M., McHardy, W.J. and Wilson, M.J. (1984a) Interstratified XRD characteristics of physical mixtures of elementary clay particles. *Clay Minerals*, **19**, 67–76.
- Nadeau, P.H., Wilson, M.J., McHardy, W.J. and Tait, J.M. (1984b) Interparticle diffraction: a new concept for interstratified clays. *Clay Minerals*, **19**, 757–769.
- Nadeau, P.H., Wilson, M.J., McHardy, W.J. and Tait, J.M. (1985) The conversion of smectite to illite during diagenesis: evidence from some illitic clays from bentonites and sandstones. *Mineralogical Magazine*, **49**, 393–400.
- Reynolds, R.C. Jr. (1992) X-ray diffraction studies of illite/smectite from rocks, <1 µm randomly oriented powders, and <1 µm oriented powder aggregates: the absence of laboratory-induced artifacts. *Clays and Clay Minerals*, **40**, 387–396.
- Środoń, J. (1981) X-ray identification of randomly interstratified illite/smectite in mixtures with discrete illite. *Clay Minerals* **16**, 297–304.
- Środoń, J. (1984) X-ray powder diffraction identification of illitic materials. *Clays and Clay Minerals*, **32**, 337–349.
- Środoń, J., Andreoli, C., Elsass, F. and Robert, M. (1990) Direct high-resolution transmission electron microscopic measurements of expandability of mixed-layer illite/smectite in bentonite rock. *Clays and Clay Minerals*, **38**, 373–379.
- Środoń, J., Eberl, D.D. and Drits, V. (2000) Evolution of fundamental particle size during illitization of smectite and implications for the illitization mechanism. *Clays and Clay Minerals*, **48**, 446–459.
- Środoń, J., Elsass, F., McHardy, W.J. and Morgan, D.J. (1992) Chemistry of illite-smectite inferred from TEM measurements of fundamental particles. *Clay Minerals*, **27**, 137–158.
- Šucha, V., Kraus, I., Gerthofferová, H., Petes, J. and Sereková, M. (1993) Smectite to illite conversion in bentonites and shales of the East Slovak Basin. *Clay Minerals*, **28**, 243–253.
- Uhlik, P., Šucha, V., Elsass, F. and Čaplovičová, M. (2000) High-resolution transmission electron microscopy of mixed-layer clays dispersed in PVP-10: A new technique to distinguish detrital and authigenic illitic material. *Clay Minerals*, **35**, 781–789.

(Received 9 July 2002; revised 21 April 2003; Ms. 675; A.E. Douglas K. McCarty)

## ANOMALOUS CONTACT M

ISABE

<sup>1</sup> D  
<sup>2</sup> Departamento de

<sup>3</sup> Departamento

### Abstract-

Spain) wa  
laccolith  
ocean flo  
Cordillera  
of grossul  
500°C. Ph  
indicating  
In the are  
chlorite is  
smectites  
laccolith  
circulation  
subvolcan  
metamorp  
rocks, and

**Key Wor**  
Hydrothe

Intrusions of sr  
rocks can provide  
thermal effects in t  
hydrothermal syst  
(Fulginiti *et al.*,  
processes of rock-  
phyllosilicates. The  
alteration of volca  
studied extensively  
and Mackinnon, 19  
*al.*, 1999) due to  
global distribution  
physical properties  
1981; Laverne, 198  
mineral assemblage  
prevailing conditio  
processes that affec  
bodies (Vitali *et a*  
corrensite and chi  
hydrothermally-alte  
have dealt pred

\* E-mail address of  
jmillan@ujaen.es  
DOI: 10.1346/CCM

Copyright © 2003, The